

# Highly Linear Temperature Sensor Based on 4H-Silicon Carbide p-i-n Diodes

Sandro Rao, *Member, IEEE*, Giovanni Pangallo, and Francesco G. Della Corte, *Member, IEEE*

**Abstract**—The linear dependence on temperature of the voltage drop difference measured on two diodes biased at different constant currents has been characterized in a range from room temperature up to 573 K. The realized proportional to absolute temperature sensor shows a good level of linearity and the corresponding rms error lower than 0.3%. Moreover, a maximum sensitivity of 610  $\mu\text{V/K}$  has been obtained, with an extrapolated output converging to 0 V at  $T = 0$  K, in agreement with theory and allowing a single-point temperature calibration.

**Index Terms**—P-i-n diodes, power semiconductor devices, silicon carbide, temperature sensors.

## I. INTRODUCTION

DIODES are the most common semiconductor devices used for temperature sensing. These sensors exploit the quasi-linear dependence on temperature of the voltage drop,  $V_D$ , across a forward-biased diode. The advantage of such devices, if compared to other sensors, *i.e.* thermistors and thermocouples [1], is the high compatibility with the integrated circuit (IC) technology and, more important, the highly linear output while preserving a high sensitivity.

Silicon carbide (SiC)-based devices generally operate at high power regimes maintaining good performances also at elevated temperatures [2]. To date, all of the high temperature sensors reported in literature exploit the dependence on temperature of the voltage drop across a single diode [3], [4] showing however a limited linearity.

In a recent work we proposed a temperature sensor based on 4H-SiC Schottky diodes [5] where the non-linear effects of the saturation current,  $I_s$ , and the diode parasitic series resistance,  $R_s$ , on the sensor characteristics were overcome through the use of a proportional-to-absolute-temperature (PTAT) configuration realized using two identical integrated diodes biased with different currents kept constant over the temperature range.

In this letter we present, for the first time to our knowledge, results about a high performance PTAT sensor fabricated integrating twin 4H-SiC p-i-n diodes biased in the exponential region of the  $I$ - $V$  characteristics where the series resistance can be considered negligible.

## II. SENSOR STRUCTURE

The 4H-SiC p-i-n diodes were fabricated and provided by CNR-Institute for Microelectronics and

Manuscript received September 6, 2015; accepted September 22, 2015. The review of this letter was arranged by Editor A. Ortiz-Conde.

The authors are with the Dipartimento di Ingegneria dell'Informazione, delle Infrastrutture e dell'Energia Sostenibile, Università degli Studi Mediterranea, Reggio Calabria 89122, Italy (e-mail: sandro.rao@unirc.it).

Color versions of one or more of the figures in this letter are available online at <http://ieeexplore.ieee.org>.

Digital Object Identifier 10.1109/LED.2015.2481721

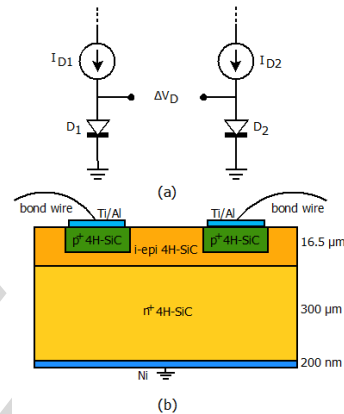


Fig. 1. (a) Electrical circuit of PTAT sensor. (b) Schematic cross section of the 4H-SiC integrated p-i-n diodes.

Microsystems (IMM), unit of Bologna (I). They were fabricated on  $\langle 0001 \rangle$   $7^\circ 62'$  off-axis 4H-SiC  $n^+$ -type homoepitaxial commercial wafers [6], with a thickness of 300  $\mu\text{m}$  and a conductivity of 0.021  $\Omega\text{-cm}$ . The epilayer is 16.5  $\mu\text{m}$  thick and has a net doping density of about  $3 \times 10^{15} \text{ cm}^{-3}$ . The corresponding fabrication process involves technological steps that are standard for microelectronic industry, ensuring reproducibility of results. In particular the circular  $p^+$ -type anode regions were obtained simultaneously by ion implantation of Al through a  $\text{SiO}_2$  mask designed to pattern the vertical p-i-n diodes with p-type area of  $7.54 \times 10^{-4} \text{ cm}^2$ . Photolithography and wet chemical etching were used to define the circular p-i-n Ti/Al top contacts. A 200 nm-thick Ni film was deposited on the back of the wafer to form the ohmic back contact. Finally, the chip was annealed in vacuum at 1000°C for 8 min. Full details about the fabrication are provided in [7] and [8].

In Fig. 1(a) the schematic equivalent circuit of the on-chip integrated PTAT sensor is shown.

The microchip contains several p-i-n diodes with the common cathode consisting of the  $n^+$  4H-SiC substrate. The chip was packaged and the Ti/Al metal contacts were bonded using thin Al wires, 50  $\mu\text{m}$  in diameter, to a custom printed circuit board (PCB) to allow an electrical connection to the measurement set-up.

A detail of the chip cross section is schematically shown in Fig. 1(b). The distance between the two devices is 190  $\mu\text{m}$ .

The chip surface was unpassivated. In an optimized design, the formation of a passivation layer should be considered to improve reliability by avoiding undesired effects such as surface oxidation and/or current cross-talk between the two diodes, however not observed in this experimental work.

In our setup, two p-i-n diodes,  $D_1$  and  $D_2$ , with almost identical  $I_D - V_D$  characteristics (root mean square error,  $\text{rmse} = 1.01 \times 10^{-5}$  calculated over the full bias range), were driven by two external and independent current sources, providing constant  $I_{D1}$  and  $I_{D2}$  currents [Fig. 1(a)] over the whole temperature range. For ease of use, it is suggested that the same scheme is replicated in practical applications, with an off-chip driving circuit, unless a current mirror-based circuit is implemented on the same substrate. The two currents are described by the analytical expression:

$$I_{D1,2} = I_{S1,2} [\exp(qV_{D1,2}/\eta_{1,2}kT) - 1] \quad (1)$$

where  $I_{S1,2}$ ,  $V_{D1,2}$  and  $\eta_{1,2}$  are the saturation current, the diode voltage drop and the ideality factor for  $D_1$  and  $D_2$ , respectively.

If the two diodes show the same ideality factor ( $\eta_1 = \eta_2 = \eta$ ), the difference between the voltage drops across the two diodes ( $V_{D2} - V_{D1}$ ) can be written from (1) as:

$$\Delta V_D = V_{D2} - V_{D1} = (kT/q)\eta \ln(I_{D2}/I_{D1}) \quad (2)$$

Eq. (2) indicates that, for a fixed  $I_{D2}/I_{D1}$  ratio, the sensor output,  $\Delta V_D$ , is ideally proportional to  $T$  if  $\eta$  is a constant. In order to have a high linearity it is therefore necessary to ensure an ideality factor that is highly stable with  $T$ . This result can be obtained by ensuring in turn that, at all temperatures, the diode operation is constantly dominated by a specific physical phenomenon. In fact, as shown in [9], four main current components are present in a SiC p-i-n diode, namely electron (hole) injection in the anode (cathode) region, electro-hole recombination in the space charge region, and recombination in the neutral part of the i-region. Each of them is characterized by a particular value of  $\eta$ . For specific current regimes, one of them can be dominant, for example the minority carrier injection, thus fixing the  $\eta$ , which therefore remains constant with  $T$  as long as the relevant physical phenomenon prevails.

The sensitivity  $S$  is the temperature derivative of the previous equation:

$$S = d\Delta V_D/dT = (k/q)\eta \ln(r) \quad (3)$$

where  $r = I_{D2}/I_{D1}$  is the current ratio. In order to enhance the sensitivity, the ratio  $r$  can be increased. Eq. (3) also predicts that  $S$  benefits from high values of the ideality factor. However  $\eta$  in excess of 3 are generally only observed in poor quality, highly resistive, diodes, for which (1) is no more valid.

### III. EXPERIMENTAL RESULTS AND DISCUSSION

The device has been tested in a thermostatic oven (Galli G210F030P) setting the reference temperature through its internal PID digital microcontroller. Two calibrated and certified resistance temperature detectors (RTDs) based on platinum wire (PT100), with an accuracy of  $\pm 0.3$  K, were placed in contact with the PCB, through a thermal conductive paint, very close to the device under test in order to monitor, during measurements, the temperature set points. Once each operating temperature was set, and the system temperature was stable for tens of minutes,

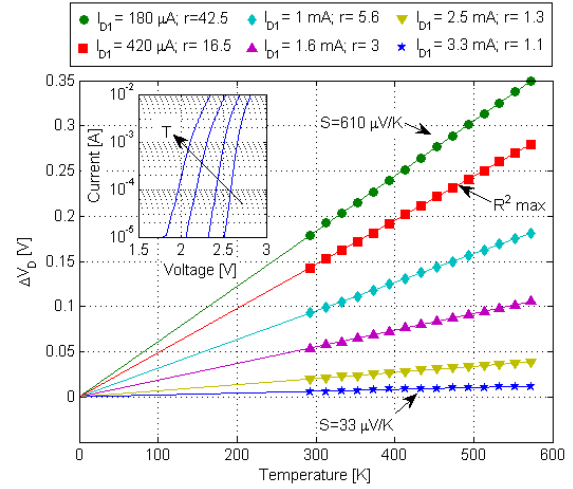


Fig. 2. Forward voltage drop difference,  $\Delta V_D$ , vs. temperature for different bias currents,  $I_{D1}$  and  $I_{D2}$ , and current ratio  $r = (I_{D2}/I_{D1})$ . The extrapolated linear fittings (straight lines) show a convergence to the origin ( $T = 0$  K and  $\Delta V_D = 0$  V) with a maximum error of  $\Delta T = \pm 0.2$  K. The inset shows the  $I-V$  characteristics in semi-log scale at four temperatures (293 K, 373 K, 473 K, 573 K).

the  $I-V$  characteristics (inset of Fig. 2) have been measured by using an Agilent 4155C Semiconductor Parameter Analyzer, in steps of  $T = 20$  K.

The forward voltage difference ( $\Delta V_D = V_{D2} - V_{D1}$ ) across the two diodes, simultaneously measured in a range from (up to)  $T = 293$  K up to (from) 573 K, is reported in Fig. 2 together with the best linear fitting. In particular, data are shown for several values of  $I_{D1}$  and  $r$ . The plot shows that  $\Delta V_D$  and  $T$  are linearly dependent each other for the whole considered temperature range. The reported corresponding sensitivities were calculated from the slope of the  $\Delta V_D$  vs.  $T$  characteristics.

In our analysis, the coefficient of determination ( $R^2$ ) [10] has been calculated to evaluate the agreement between the experimental measurements and their linear best-fit. In particular,  $R^2$  allowed us to quantify the sensor linearity goodness by fitting the experimental data with a linear model.

The experimental characteristics show a good degree of linearity ( $R^2 > 0.999$ ) for  $I_{D1}$  ranging from 180  $\mu\text{A}$  up to 3.3 mA, with  $1.1 < r < 42.5$ .

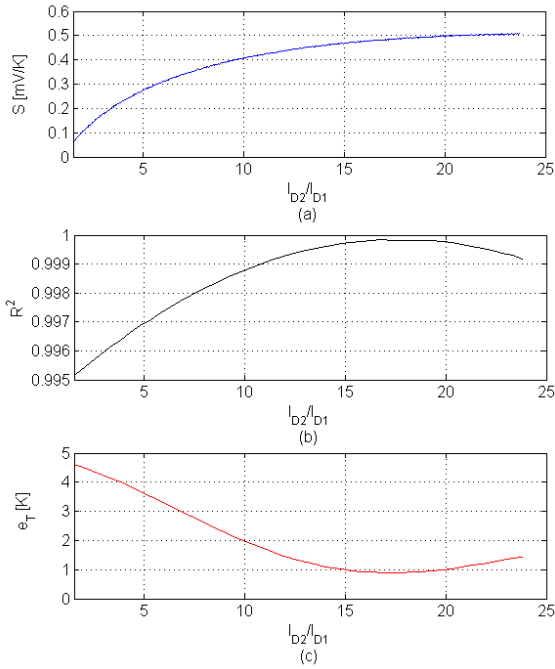
On the other hand, the sensitivity is lowest for  $I_{D1} = 3.3$  mA and  $r = 1.1$ , ( $S = 33.1 \pm 0.9$   $\mu\text{V/K}$ ) and increases for higher  $r$  in agreement with (3). For  $I_{D1} = 180$   $\mu\text{A}$  and  $r = 42.5$  we get the highest sensitivity ( $S = 610.2 \pm 0.5$   $\mu\text{V/K}$ ).

Moreover, all the  $\Delta V_D$  vs.  $T$  characteristics converge, with a very high degree of precision, to  $T = 0$  K for  $\Delta V_D = 0$  V (2). The extrapolated value of the voltage difference across the forward biased diodes,  $D_1$  and  $D_2$ , at  $T = 0$  K is in fact  $\pm 20$   $\mu\text{V}$  corresponding to a temperature error of  $\Delta T = \pm 0.2$  K.

The proposed PTAT sensor can be therefore calibrated in a single temperature point thanks to the linear behavior of  $\Delta V_D$  vs.  $T$  characteristics crossing the origin of the axes.

TABLE I  
 DIODE IDEALITY FACTOR

$I_{D1}$	$I_{D2}$	$\eta + \Delta\eta(T)$
180 $\mu\text{A}$	7.7 mA	2.01 $\pm$ 0.03
420 $\mu\text{A}$	6.9 mA	2.08 $\pm$ 0.01
1 mA	5.6 mA	2.22 $\pm$ 0.01
1.6 mA	4.7 mA	2.27 $\pm$ 0.01
2.5 mA	3.2 mA	2.28 $\pm$ 0.02
3.3 mA	3.6 mA	2.49 $\pm$ 0.02

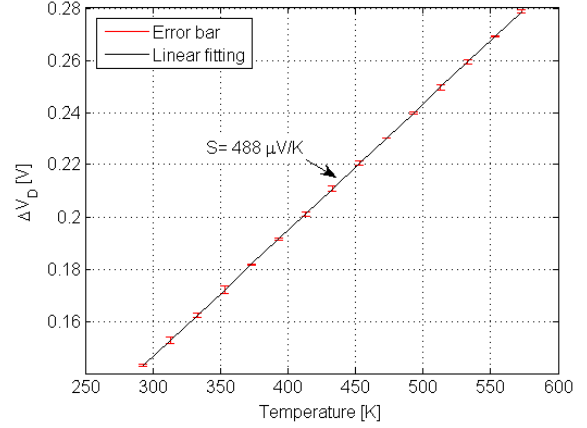

 Fig. 3. Sensitivity (a), coefficient of determination (b), and rmse for the whole temperature range of 293-573 K (c) vs. current ratio for  $I_{D1} = 420 \mu\text{A}$ .

162 This is a clear advantage of PTAT sensors with respect to  
 163 those based on a single diode, widely used in particular for  
 164 high temperature sensing [2], [3].

165 In our analysis, the diode ideality factor was calculated from  
 166 the slope of the  $\ln(I_D) - V_D$  linear fitting over the bias current  
 167 ranges considered in Fig. 2. In Table I we summarize the  
 168 calculated  $\eta(T)$  valid for the temperature range  $T = 293 \text{ K}$   
 169 up to 573 K, in good agreement with (3). It is worth noting  
 170 that the maximum variation of  $\eta$  with  $T$  in the considered  
 171 current range ( $I_{D1} = 180 \mu\text{A}$ ,  $I_{D2} = 7.7 \text{ mA}$ ) is 1.5% leading  
 172 therefore to a highly linear temperature sensor.

173 To evaluate the mismatch between the calculated linear  
 174 best-fit and the experimental measurements, the rmse was  
 175 first calculated and subsequently converted into a temperature  
 176 error.

177 A detailed analysis of the device performance is shown  
 178 in Fig. 3, where the sensitivity,  $S$ , the coefficient of deter-  
 179 mination,  $R^2$ , and the corresponding average error for the  
 180 considered temperature range,  $e_T$ , is shown for different values  
 181 of the current ratio,  $r$ , and for a bias current  $I_{D1}$  of 420  $\mu\text{A}$ .


 Fig. 4. Linear fit and rms error bar of  $(V_{D2} - V_{D1})$  vs.  $T$  for the four diode pairs. The five measurement cycles, from (up to) 293 K up to (from) 543 K, were done in different days. The bias currents are the same for all PTAT sensors,  $I_{D1} = 420 \mu\text{A}$  and  $I_{D2} = 6.9 \text{ mA}$ .

As  $r$  increases the PTAT sensor output exhibits a much higher  
 182 sensitivity in agreement with (3). 183

For  $r = 16.5$  ( $I_{D2} = 6.9 \text{ mA}$ ),  $e_T$  reaches its minimum,  
 184  $e_T = 0.9 \text{ K}$ , corresponding to 0.3% over the whole tempera-  
 185 ture range. 186

It is worth noting that our sensor shows a very good  
 187 linearity, always above  $R^2 = 0.995$ , with an average value  
 188 of 0.9984 and a standard deviation of 0.0015. 189

Finally, four different couples of diodes, from two dif-  
 190 ferent microchips, were characterized to evaluate the sensor  
 191 reproducibility by iteratively repeating for five times the  
 192 same cycles of measurements, from (up to) 293 K up to  
 193 (from) 543 K, also in different days. Results are summarized  
 194 in Fig. 4, for  $I_{D1} = 420 \mu\text{A}$ , and led to a calcula-  
 195 ted mismatch among the different sensors always lower  
 196 than  $\pm 1.1\%$ . Moreover, the coefficient of determination is  
 197  $R^2 = 0.9997 \pm 2 \times 10^{-4}$  and the corresponding sensitivity  
 198 is  $S = 494 \mu\text{V/K}$  with a standard deviation of 13  $\mu\text{V/K}$ . 199

#### IV. CONCLUSION

200 In this letter, a PTAT sensor based on integrated  
 201 4H-SiC p-i-n diodes was characterized. Measurements showed  
 202 both a very good degree of linearity and a high sensitivity  
 203 ( $S = 610 \mu\text{V/K}$ ) in the temperature range 293-573 K. 204

The proposed PTAT sensor output is independent of the sat-  
 205 uration current, has the advantage of being calibratable in just  
 206 one temperature point and shows a good repeatability main-  
 207 taining a stable output over different cycles of measurements. 208

#### ACKNOWLEDGMENT

209 Dr. Nipoti Roberta from CNR-IMM-UOS Unit of  
 210 Bologna (Italy) is gratefully acknowledged for providing the  
 211 p-i-n diodes and for helpful discussions. 212

#### REFERENCES

- 213 [1] J. P. Bentley, "Temperature sensor characteristics and measurement  
 214 system design," *J. Phys. E, Sci. Instrum.*, vol. 17, no. 6, 1984. 215  
 216 DOI: 10.1088/0022-3735/17/6/002 216 AQ:2



- 217 [2] C. Buttay, C. Raynaud, H. Morel, G. Civrac, M.-L. Locatelli,  
218 and F. Morel, "Thermal stability of silicon carbide power diodes,"  
219 *IEEE Trans. Electron Devices*, vol. 59, no. 3, pp. 761–769, Mar. 2012.  
220 DOI: 10.1109/TED.2011.2181390
- 221 [3] N. Zhang, C.-M. Lin, D. G. Senesky, and A. P. Pisano, "Temper-  
222 ature sensor based on 4H-silicon carbide pn diode operational from  
223 20 °C to 600 °C," *Appl. Phys. Lett.*, vol. 104, no. 7, p. 073504, Feb. 2014.  
224 DOI: 10.1063/1.4865372
- 225 [4] G. Brezeanu, F. Draghici, F. Craciunoiu, C. Boianeanu, F. Bernea,  
226 F. Udrea, D. Puscasu, and I. Rusu, "4H-SiC Schottky diodes  
227 for temperature sensing applications in harsh environments,"  
228 *Mater. Sci. Forum*, vols. 679–680, pp. 575–578, Mar. 2011.  
229 DOI: 10.4028/www.scientific.net/MSF.679-680.575
- 230 [5] S. Rao, G. Pangallo, F. Pezzimenti, and F. G. D. Corte, "High-  
231 performance temperature sensor based on 4H-SiC Schottky diodes,"  
232 *IEEE Electron Device Lett.*, vol. 36, no. 7, pp. 720–722, Jul. 2015.  
233 DOI: 10.1109/LED.2015.2436213
- 234 [6] Cree Research Inc., Durham, NC, USA. [Online]. Available:  
235 <http://www.cree.com/power>
- 236 [7] F. G. D. Corte, F. Pezzimenti, and R. Nipoti, "Simulation  
237 and experimental results on the forward  $J$ - $V$  characteristic of  
238 Al implanted 4H-SiC p-i-n diodes," *Microelectron. J.*, vol. 38,  
239 no. 12, pp. 1273–1279, Dec. 2007. DOI: 10.1016/j.mejo.  
240 2007.09.024
- 241 [8] A. Poggi, F. Bergamini, R. Nipoti, S. Solmi, M. Canino, and  
242 A. Carnera, "Effects of heating ramp rates on the character-  
243 istics of Al implanted 4H-SiC junctions," *Appl. Phys. Lett.*,  
244 vol. 88, no. 16, pp. 162106–162109, Apr. 2006. [Online]. Available:  
245 <http://dx.doi.org/10.1063/1.2196233>
- 246 [9] S. Bellone, F. G. D. Corte, L. F. Albane, and F. Pezzime,  
247 "An analytical model of the forward  $I$ - $V$  characteristics of  
248 4H-SiC p-i-n diodes valid for a wide range of temperature  
249 and current," *IEEE Trans. Power Electron.*, vol. 26, no. 10,  
250 pp. 2835–2843, Oct. 2011. DOI: 10.1109/TPEL.2011.  
251 2129533
- 252 [10] N. J. D. Nagelkerke, "A note on a general definition of the coefficient  
253 of determination," *Biometrika*, vol. 78, no. 3, pp. 691–692, Sep. 1991.  
254 DOI: 10.1093/biomet/78.3.691

IEEE  
PROOF